



# Integrated Synchronization Control of Grid-Forming Inverters for Smooth Microgrid Transition

## Preprint

Jing Wang, Annabelle Pratt, and Murali Baggu

*National Renewable Energy Laboratory*

*Presented at the 2019 IEEE Power and Energy Society General Meeting (IEEE PES GM)*

*Atlanta, Georgia*

*August 4–8, 2019*

**NREL is a national laboratory of the U.S. Department of Energy  
Office of Energy Efficiency & Renewable Energy  
Operated by the Alliance for Sustainable Energy, LLC**

This report is available at no cost from the National Renewable Energy Laboratory (NREL) at [www.nrel.gov/publications](http://www.nrel.gov/publications).

Contract No. DE-AC36-08GO28308

**Conference Paper**  
NREL/CP-5D00-72756  
November 2019



# Integrated Synchronization Control of Grid-Forming Inverters for Smooth Microgrid Transition

## Preprint

Jing Wang, Annabelle Pratt, and Murali Baggu

*National Renewable Energy Laboratory*

### Suggested Citation

Wang, Jing, Annabelle Pratt, and Murali Baggu. 2019. *Integrated Synchronization Control of Grid-Forming Inverters for Smooth Microgrid Transition: Preprint*. Golden, CO: National Renewable Energy Laboratory. NREL/CP-5D00-72756.

<https://www.nrel.gov/docs/fy20osti/72756.pdf>.

© 2019 IEEE. Personal use of this material is permitted. Permission from IEEE must be obtained for all other uses, in any current or future media, including reprinting/republishing this material for advertising or promotional purposes, creating new collective works, for resale or redistribution to servers or lists, or reuse of any copyrighted component of this work in other works.

**NREL is a national laboratory of the U.S. Department of Energy  
Office of Energy Efficiency & Renewable Energy  
Operated by the Alliance for Sustainable Energy, LLC**

This report is available at no cost from the National Renewable Energy Laboratory (NREL) at [www.nrel.gov/publications](http://www.nrel.gov/publications).

Contract No. DE-AC36-08GO28308

**Conference Paper**  
NREL/CP-5D00-72756  
November 2019

National Renewable Energy Laboratory  
15013 Denver West Parkway  
Golden, CO 80401  
303-275-3000 • [www.nrel.gov](http://www.nrel.gov)

## NOTICE

This work was authored in part by the National Renewable Energy Laboratory, operated by Alliance for Sustainable Energy, LLC, for the U.S. Department of Energy (DOE) under Contract No. DE-AC36-08GO28308. Funding provided by U.S. Department of Energy Office of Electricity Delivery and Energy Reliability. The views expressed herein do not necessarily represent the views of the DOE or the U.S. Government. The U.S. Government retains and the publisher, by accepting the article for publication, acknowledges that the U.S. Government retains a nonexclusive, paid-up, irrevocable, worldwide license to publish or reproduce the published form of this work, or allow others to do so, for U.S. Government purposes.

This report is available at no cost from the National Renewable Energy Laboratory (NREL) at [www.nrel.gov/publications](http://www.nrel.gov/publications).

U.S. Department of Energy (DOE) reports produced after 1991 and a growing number of pre-1991 documents are available free via [www.osti.gov](http://www.osti.gov).

*Cover Photos by Dennis Schroeder: (clockwise, left to right) NREL 51934, NREL 45897, NREL 42160, NREL 45891, NREL 48097, NREL 46526.*

NREL prints on paper that contains recycled content.

# Integrated Synchronization Control of Grid-Forming Inverters for Smooth Microgrid Transition

Jing Wang, Annabelle Pratt, Murali Baggu

Power Systems Engineering Center, National Renewable Energy Laboratory Golden, CO 80401, USA  
[jing.wang@nrel.gov](mailto:jing.wang@nrel.gov), [annabelle.pratt@nrel.gov](mailto:annabelle.pratt@nrel.gov), [murali.baggu@nrel.gov](mailto:murali.baggu@nrel.gov)

**Abstract**—This paper develops an integrated synchronization control technique for a grid-forming inverter operating within a microgrid that can improve the microgrid’s transients during microgrid transition operation. This integrated synchronization control includes the disconnection synchronization control and the reconnection synchronization control. The simulation results show that the developed synchronization control works effectively to smooth the angle change of the grid-forming inverter during microgrid transition operation. Thus, the microgrid’s transients are significantly improved compared to the case without synchronization control.

**Index Terms**— Disconnection Synchronization Control; Integrated Synchronization Control; Microgrid Transition Operation; Reconnection Synchronization Control.

## I. INTRODUCTION

A distributed renewable energy-powered microgrid is becoming feasible especially with increasing numbers of storage units installed [1]. A basic functional requirement for microgrid is the capability to transition between grid-connected and islanded mode if needed. Because there is no synchronous machine type of generation working as the grid-forming source in this type of microgrid when islanded, at least one inverter-interfaced distributed energy resource (DER) (e.g., battery) is assigned as the grid-forming source to form the stiff bus voltage in an islanded microgrid [2].

The grid-forming source plays an important role in ensuring smooth transition operation. From islanded to grid-connected mode, the grid-forming source adjusts its output voltage and frequency to meet the reconnection criteria (differences in voltage, frequency, and phase angle between the grid voltage and the microgrid voltage at the point of common coupling (PCC) within the thresholds), thus reconnecting to the main grid with smooth transients [3]. Extensive research has been done to achieve synchronization and smooth reconnection operation, such as [4] – [6].

However, the synchronization from grid-connected to islanded mode is overlooked. The commonly accepted strategy for smooth disconnection operation is to have “zero” active and reactive power at the PCC during the disconnection. But because the grid-forming source follows its own frequency when the microgrid transitions to islanded mode, there might be a phase jump if a synchronization control technique is not used. This causes harmful transients in voltage and current when the microgrid disconnects from the main grid. Therefore, smooth transients during disconnection also rely on synchronization between the PCC microgrid voltage and the startup voltage of the grid-forming source when the microgrid becomes islanded.

Because of the inertia in the rotating mass of a synchronous machine, there is no phase jump during microgrid transition operation if a synchronous machine is used as a grid-forming source [7]. A universal integrated synchronization control

technique mimicking the dynamics of a synchronous generator is proposed in [7] to achieve smooth transients (phase synchronization) during microgrid transition operation. Some similar conceptual works aim to construct the dynamics of a virtual synchronous machine as well [8] – [9]; however, the complexity and computational burden might limit their applications in a real inverter controller. Moreover, coordination among the microgrid controller, PCC circuit breaker controller, and inverter controller is not investigated properly. Therefore, this paper presents a practical synchronization control technique of grid-forming inverter(s) coordinating with the PCC circuit breaker controller and the microgrid controller to achieve phase synchronization during microgrid transition operation (from grid-connected to islanded mode and vice versa).

The contribution of this paper is to (1) provide comprehensive analysis of the synchronization mechanism for a grid-forming inverter, (2) design an integrated synchronization control technique in the grid-forming inverter to achieve smooth transients for various microgrid transition operations, and (3) present the detailed design and implementation as a good example or reference for replication by those researching microgrid smooth transition operation.

## II. CONTROL STRATEGY FOR GRID-FORMING INVERTER FOR SMOOTH MICROGRID TRANSITION OPERATION

From the control point of view, transients are caused by changes in the state variables  $u$  (e.g., voltage and current). Thus, smooth transition operation can be achieved by minimizing changes in the state variables prior to and after transition operation ( $u_- = u_+$ ) [2]. Following this strategy and an in-depth understanding of the grid-forming inverter control, two fundamental requirements should be included in the grid-forming inverter control: a fixed control structure (using voltage control in both grid-connected and islanded modes) and a fixed phase angle for the Park transformation (no/minimal change in the phase angle prior to and after transition operation). As a result, the system transients are minimized, and the impact on the whole network, especially sensitive loads, can be reduced, thus achieving smooth and safe transition between the modes.

### A. Fixed Control Structure

Typically, active and reactive power (PQ) control is adopted by all the DER units if no ancillary service is required in grid-connected mode. The commanded power reference ( $P^*$  and  $Q^*$ ) is used to calculate the current reference for the inner current control loop. The current control is used because the output voltage of the DER is governed by the grid voltage, so the voltage control loop fails to offer sound and accurate control [3]. For the islanded mode, the grid-forming inverter uses voltage and frequency (VF) control to form the stiff bus voltage, and other DERs continue the PQ control. Therefore, it is necessary to reconfigure the control structure (between the current and

voltage control) of the grid-forming inverter during microgrid transition operation.

To implement voltage control in both grid-connected and islanded modes, the injected current can be indirectly controlled by controlling the inverter terminal voltage if an impedance exists between the grid and the voltage terminal (to be controlled) of the inverter because the impedance is a given parameter and the grid voltage is an exogenous observable variable. Or a virtual output impedance can be introduced to emulate the physical impedance and thus control the terminal voltage of an inverter in grid-connected mode. But the complexity of the control algorithm increases; thus, a practical voltage control algorithm developed in [10] is used as the control algorithm for an inverter for both grid-connected and islanded modes.

### B. Fixed Phase Angle: Synchronization Control

The strategies to achieve synchronization control fall into two main categories: (1) emulate the dynamics of a synchronous machine to add virtual inertia to the system (i.e., synchroconverter/synchronous converter), and (2) control the phase angle directly. Both approaches are applicable to achieve synchronization control because of the high controllability of the power converters. The second approach is more straightforward and does not require special knowledge of the synchronous machine. Therefore, the second approach is adopted in this paper.

## III. DESIGN OF THE INTEGRATED SYNCHRONIZATION CONTROL FOR GRID-FORMING INVERTER

### A. Mechanism of Synchronization Control

In islanded mode, the grid-forming inverters are controlled as an ideal voltage source with a given amplified  $E^*$  and frequency  $\omega^*$  [3]. For a system with a single grid-forming inverter,  $E^*$  and  $\omega^*$  can be set as nominal values. If there are multiple grid-forming inverters, droop control is usually used to generate the common  $E^*$  and  $\omega^*$  references for all grid-forming inverters for power sharing. In grid-connected mode, the grid-forming inverters change to grid-feeding or grid-supporting inverters depending on the network condition. Because the grid-feeding function is the more commonly used control strategy for grid-connected inverters, here we discuss only the grid-feeding inverter when the microgrid is grid-connected.

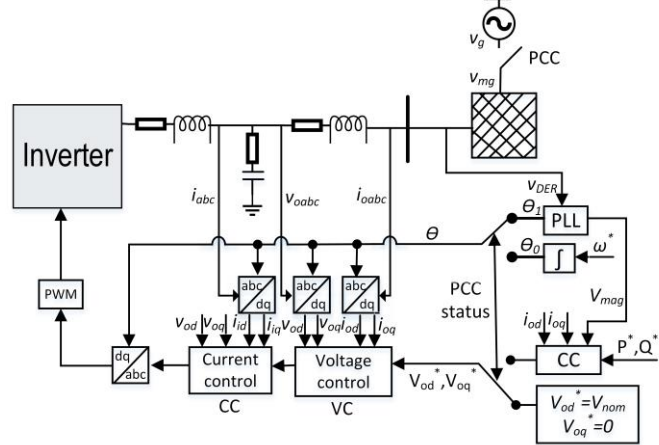


Fig. 1. Schematic diagram of the control algorithm for grid-forming and grid-feeding inverters.

As discussed in the previous section, it is necessary to have the same control structure working for both the grid-forming and grid-feeding inverters. Fig. 1 outlines the general form of an inverter-level control algorithm, which has the same control structure for grid-forming and grid-feeding inverters. The outer loop is the voltage control (VC), and the inner loop is the current control (CC). The implementation is performed in a

synchronous frame, and the angle  $\theta$  is generated for the Park Transformation. In grid-connected mode, the PCC status is “1”. The angle  $\theta_i$  is selected, and the voltage references ( $V_{od}^*$ ,  $V_{oq}^*$ ) for the VC are generated based on the power reference,  $P^*$ ,  $Q^*$ ; the voltage magnitude,  $V_{mag}$ , of the connection point voltage,  $v_{DER}$ ; and the inverter output current,  $i_{od}$  and  $i_{oq}$ . For the equations of CC to calculate the voltage references, refer to [10]. In islanded mode, the PCC status is “0”. The angle  $\theta_0$  is selected, and the voltage references are fixed values if droop control is not used.  $V_{nom}$  is the nominal voltage magnitude of the inverter. When the microgrid operation mode is changed, the adjustments of the inverter control algorithm are the angle  $\theta$  for the Park transformation and voltage references,  $V_{od}^*$  and  $V_{oq}^*$ . The changes in the voltage references are unavoidable because the control objectives in the application/system level are different for grid-forming and grid-feeding inverters, and the power references ( $P^*$ ,  $Q^*$ ) are determined by a microgrid controller. Therefore, we focus only on the angle  $\theta$  to avoid any changes and have smooth transition operation.

Fig. 1 shows that four blocks need the angle information, which reveals that the angle  $\theta$  significantly affects the dynamics and stability of the inverter’s controller. The value of  $\theta_i$  is generated by the inverter’s connecting voltage,  $v_{DER}$ , by using a phase-locked loop (PLL) and  $\theta_0$  is generated by a fixed frequency reference,  $\omega^*$ , integrated with time. To have smooth transients in  $\theta$  when the microgrid changes operation mode, the rule of thumb is to make  $\theta_i \approx \theta_0$ . This also indicates the “synchronization” control in this paper. Because of the grid-following feature of the grid-feeding inverter, the flexibility lies in the grid-forming inverter. Further, the angle augment must be implemented differently from grid-connected to islanded mode and vice versa because the angle  $\theta_0$  does not take effect until the microgrid switches from grid-connected to islanded mode and the angle  $\theta_0$  is already used from islanded to grid-connected mode.

### B. Development of the Synchronization Control

The development of the synchronization control technique for disconnection and reconnection is carried out separately. Also, coordination among signals is necessary to allow automatic operation for various transition operation scenarios. The overall design schematics of the synchronization control are presented in Fig. 2, which includes coordination among the signals, disconnection synchronization control, and reconnection synchronization control.

#### 1) Coordination

This block is essential to make the synchronization control work because it triggers the right synchronization block at the right time and sends out the correct augmented angle  $\theta_0$ . The transition and steady-state signals are received from the microgrid transition controller. According to [11], the meaning of these two signals are as listed in Table 1. When the microgrid is grid-connected, the values of the steady-state and transition modes are 0, so  $\Delta\theta$  is 0. In disconnection, the transition value is “2” and “Enable1” is high, so the output of the disconnection synchronization control will be selected. During islanded mode, the angle from the disconnection control will be set as the initial angle. In reconnection, the transition value is “1” and “Enable2” is high, so the output of the reconnection synchronization control will be chosen. To ensure continuity, this angle will be added with the angle from the steady-state islanded mode. Note that the enable signal will be disabled when the PCC circuit breaker takes the expected action.

Scenario	Steady State	Transition	Enable
Grid-connected	1	0	N/A

Disconnection	1	2	Enable1
Islanded	0	0	N/A
Reconnection	0	1	Enable2

## 2) Disconnection synchronization control

When the microgrid disconnects from the main grid, there are a few ways to force  $\theta_0$  to approach  $\theta_I$ : (1) add the angle difference ( $\varphi = \theta_I - \theta_0$ ) to the angle  $\theta_0$  directly; (2) check the angle difference  $\varphi$ , if it is within the threshold, and disconnect the microgrid; and (3) combine 1 and 2 to diminish the angle difference between  $\theta_I$  and  $\theta_0$  for disconnection, similar to the active synchronization control used to transition from islanded to grid-connected mode. The third option is selected, and the design is shown in Fig. 2, marked in the upper grey box.

“Enable1” is the signal generated in the microgrid transition control to initialize the disconnection check block in the PCC circuit breaker control and to enable the synchronization control in the grid-forming inverters. The disconnection synchronization control block operates only when the disconnection action is initialized by the microgrid transition controller. The inputs are the three-phase voltage,  $v_{DER}$ , and the voltage magnitude, “1”, and the output of the disconnection synchronization control is the compensation angle,  $\Delta\theta_{com1}$ . This angle will be added with  $\theta_0$  to get the new angle for the grid-forming inverter. Inside the disconnection synchronization block,  $v_{DER}$  is per unitized first as  $v'_{DER}$ , and the grid-forming inverter’s three-phase voltage,  $v'_{o}$ , is also constructed with the angle of the compensation angle,  $\Delta\theta_{com1}$ . The angle of  $v_{DER}$  is  $\theta_I$ , the angle of the three-phase voltage source is  $\theta_0$ , the angle difference between them is  $\varphi$  ( $\varphi = \theta_I - \theta_0$ ). We have the following calculation:

$$\begin{cases} v'_{DER,a}v'_{o,a} + v'_{DER,b}v'_{o,b} + v'_{DER,c}v'_{o,c} = \frac{3}{2}\cos(\varphi) = m \\ v'_{DER,a}v'_{o,b} + v'_{DER,b}v'_{o,c} + v'_{DER,c}v'_{o,a} = -\frac{3}{4}\cos(\varphi) - \frac{3\sqrt{3}}{4}\sin(\varphi) = n \end{cases}$$

Then we have  $\sin(\varphi)$  and  $\cos(\varphi)$ , calculated as:

$$\begin{cases} \cos(\varphi) = \frac{2}{3}m \\ \sin(\varphi) = \frac{-2m-4n}{3\sqrt{3}} \end{cases}$$

Based on the signs and values of  $\sin(\varphi)$  and  $\cos(\varphi)$ , the angle difference,  $\varphi$ , can be calculated and integrated to allow the angle difference to be compensated continuously. The integrated angle difference is then the final compensation angle we are searching for. Note that this angle output must be “held” when the disconnection synchronization block is disabled. Thus, the grid-forming inverter can use this angle as the initial angle when the microgrid transitions to islanded mode.

## 3) Reconnection synchronization control

For the reconnection synchronization control, the inputs are the three-phase grid-side voltage at the PCC,  $v_g$ , and the voltage of the grid-forming inverter,  $v_{oabc}$ ; and the output is the compensation angle,  $\Delta\theta_{com2}$ . The two three-phase voltages,  $v_g$  and  $v_{oabc}$ , are per unitized. Equation (1) and (2) are used to calculate  $\sin(\varphi)$  with  $\varphi = \theta_{v_g} - \theta_{v_{oabc}}$ . When the angle,  $\varphi$ , is small,  $\sin(\varphi) \approx \varphi$ . A proportional integral control is used to regulate the angle difference,  $\varphi$ . The proportional gain is 1, and the integration gain is 5.

The grid-side voltage is used as the angle reference for the inverter to approach. But the goal is to let the angle of the inverter’s output voltage increase/decrease toward the angle of the grid voltage, not to make it equal to the angle of the grid voltage; smooth reconnection is achieved when the angle difference between the grid voltage,  $v_g$ , and the microgrid voltage,  $v_{mg}$ , is very small. In the PCC circuit breaker controller, there is one function block to check the conditions for reconnection (the voltage magnitude, frequency, and phase angle between the main grid voltage and microgrid voltage at the PCC are within the thresholds). If the conditions are met, the PCC circuit breaker is then closed. The reconnection synchronization control block is then disabled because the signal “Enable2” will be low. The output  $\Delta\theta_{com2}$  will be reset to “zero”. If the angle of  $v_{mg}$  is close to the angle of  $v_g$ , the angle  $\theta_0$  is close to  $\theta_I$  when the PCC is closed because the angle difference between  $v_g$  and  $v_{oabc}$  is the almost the same as the angle difference between  $v_{mg}$  and  $v_{DER}$  when the PCC is closed. Note that we do not know the  $\theta_I$  before reconnection, and we can know  $v_g$ . Because of the network between the inverter and the PCC, there will be a noticeable angle difference between  $v_g$  and  $v_{oabc}$ .

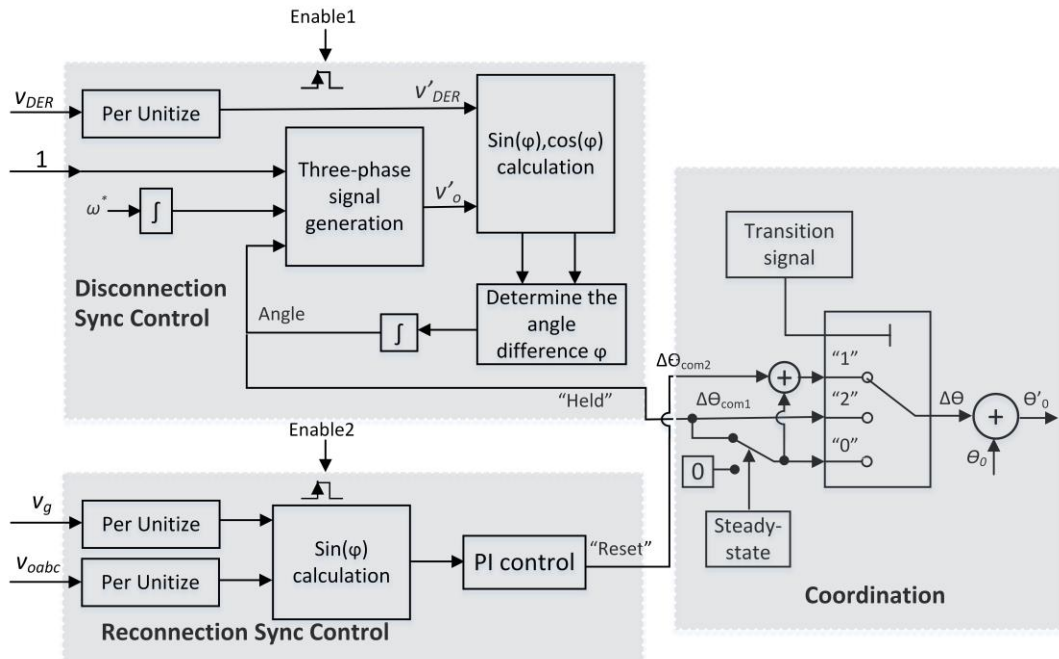


Fig. 2. Schematic diagram of the Integrated Synchronization Control of the Grid-forming source.

#### IV. SIMULATION RESULTS

To verify the proposed synchronization control, numerical simulation is performed in MATLAB/Simulink. The example microgrid model is taken from reference [2], which is a 100% renewable microgrid with two battery energy storage systems (BESSs), two photovoltaic (PV) units, commercial building loads, and residential loads. The BESS 1 works as the grid-forming source when the microgrid is islanded, and all other DERs (PV and BESS 2) work as grid-feeding sources. For the low-level inverter control algorithm shown in Fig. 1, refer to [10]. Two cases are studied to verify the design: disconnect the microgrid from the main grid, and reconnect the microgrid to the main grid. For each case, the results without synchronization control are presented first for comparison.

##### A. Test Case 1: Disconnect from the Main Grid

In this test case, the microgrid performs intentional islanding at 6 s. The steady-state value remains “1”, and the transition signal changes from “0” to “2” during the disconnection. As described in [11], when the active and reactive power at the PCC are lower than a certain limit (5 kW and 5 kVar, respectively), the PCC circuit breaker will be “open” for the case without disconnection synchronization control. For the case with synchronization control, one more condition (the angle difference,  $\phi$ , is smaller than a limit) is added to open the circuit breaker.

Test results without the disconnection synchronization control are presented in Fig. 3. After the microgrid is disconnected, the grid voltage,  $v_{DER}$ , is formed by the grid-forming inverter BESS 1, and we can see the abrupt change of its angle without synchronization control. This is because of the direct switch from  $\theta_I$  to  $\theta_O$  in the grid-forming source when the PCC circuit breaker is opened. The microgrid three-phase voltage  $v_{mg}$ , exhibits an abrupt angle change as well, which causes significant transients during the disconnection process. The grid-forming inverter’s output voltage,  $v_o$ , is also shown, which exhibits worse transients compared to the microgrid-side voltage  $v_{mg}$  because it is the source of transients/dynamics.

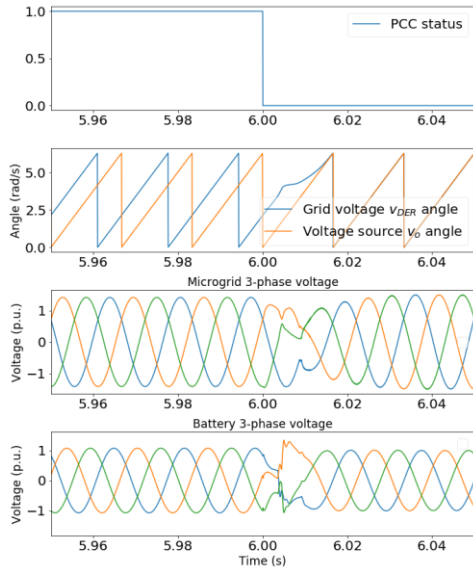


Fig. 3. Without disconnection synchronization control: PCC status, angle of the grid voltage  $v_{DER}$  and voltage source  $v_o$ , microgrid voltage, and BESS 1 output voltage.

The results with disconnection synchronization control are shown in Fig. 4. As shown in the second figure from the top in Fig. 4, the angle difference between  $v_{DER}$  and  $v_o$  is adjusted to have the angle of the voltage source  $\theta_O$  the same as the angle of the grid-following voltage  $\theta_I$ . This achieves the angle continuity of  $v_{DER}$ , which ensures smooth transients when the

microgrid is disconnected. The third figure shows the enable signal “Enable1” and the compensated angle  $\Delta\theta_{com1}$ . When the signal “Enable1” is high, the disconnection synchronization control starts to operate, and the accumulated angle difference is calculated. Because the angle difference is within a threshold, the PCC circuit breaker is open and the “Enable1” returns to low. In-line with the design, the output  $\Delta\theta_{com1}$  is kept “held”, and this angle will be the initial angle for the islanded mode. The three-phase microgrid voltage,  $v_{mg}$ , presented in the fourth figure exhibits very smooth transients, and the same applies for the output voltage of the grid-forming inverter,  $v_o$ .

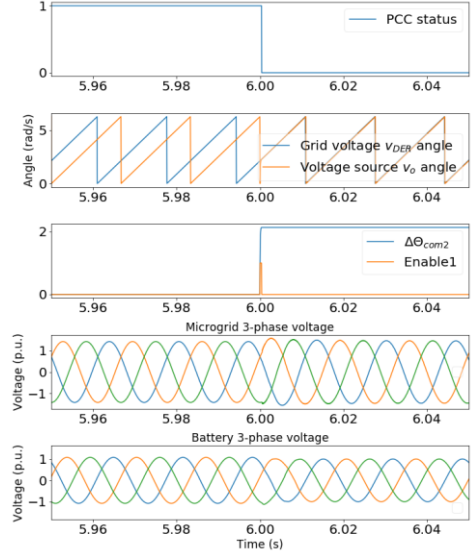


Fig. 4. With disconnection synchronization control: PCC status, angle of the grid voltage and voltage source, angle compensation, microgrid voltage, and BESS 1 output voltage.

The simulation results for the case without and with the disconnection synchronization control clearly demonstrate significant improvements in the system’s transients with disconnection synchronization control. This also shows that the smooth angle change in the grid-forming inverters is key to having smooth transients for the grid-forming inverter itself and for the rest of the system in an islanded microgrid during microgrid disconnection.

##### B. Test Case 2: Reconnect to the Main Grid

In this test case, the microgrid is requested to reconnect to the main grid between 5 and 9 s. If the reconnection criteria are not met, the microgrid reconnects to the main grid at 9 s.

Test results without reconnection synchronization control are shown in Fig. 5. Because the angle difference between the microgrid voltage,  $v_{mg}$ , and the main grid,  $v_g$ , is bigger than the angle defined in the reconnection criteria, the microgrid is not able to be reconnected at the defined time slot (between 5 and 9 s), and it is reconnected at 9 s, as designed. As shown in the second and the third figures in Fig. 5, there is a nonnegligible angle difference between  $v_{mg}$  and  $v_g$ . When the PCC circuit breaker is closed, the microgrid voltage,  $v_{mg}$ , quickly follows the main grid voltage,  $v_g$ , and no obvious transients are observed. For the grid-forming inverter, the transition transients are significant and harmful, and the voltage magnitude exhibits significant overshoot.

The results with reconnection synchronization control are shown in Fig. 6. The first figure shows that the PCC circuit breaker is closed around 5.175 s. The second figure shows that the angle difference between  $v_{mg}$  and  $v_g$  reduces gradually after 5 s and becomes almost zero before the PCC circuit breaker is closed. The third figure shows the enable signal “Enable2” and the compensated angle,  $\Delta\theta_{com2}$ . When the signal “Enable2” is high, the reconnection synchronization control starts to operate, and the compensated angle,  $\Delta\theta_{com2}$ , is calculated. The fourth

figure shows Phase A of the microgrid voltage,  $v_{mga}$ , and the main grid voltage,  $v_{ga}$ , from the beginning of the reconnection synchronization control to the closing of the PCC circuit breaker. Once the synchronization control block starts to operate, the angle difference between the microgrid and the main grid starts to reduce gradually. After a few cycles, the two signals are in phase. At 5.165 s, the angle difference between the main grid and the microgrid is within the predefined threshold, and other conditions are met as well, and the PCC circuit breaker is then closed. This also disables the enable signal “Enable2”, and the compensate angle is then reset. The waveforms of the microgrid voltage,  $v_{mga}$ , and the three-phase voltage of the grid-forming inverter BESS 1,  $v_{oabc}$ , exhibit smooth transients when the PCC circuit breaker is closed.

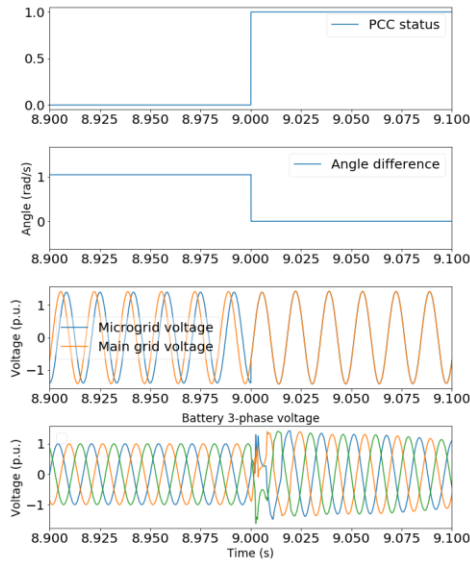


Fig. 5. Results without reconnection synchronization control: PCC status, angle of the grid voltage and voltage source, microgrid three-phase voltage, and BESS 1 output voltage.

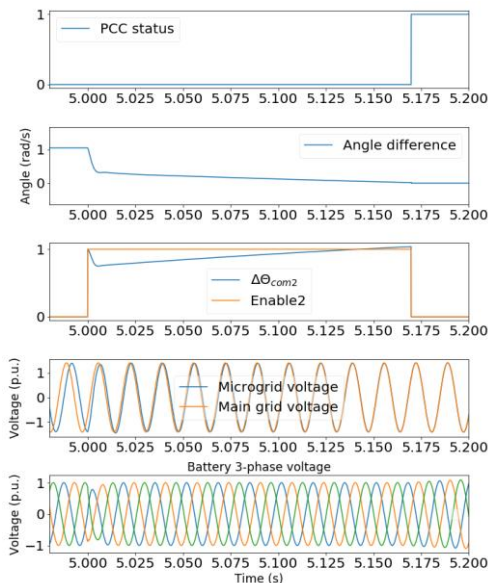


Fig. 6. Results with reconnection synchronization control: PCC status, angle of the grid voltage and voltage source, microgrid three-phase voltage, and BESS 1 output voltage.

The simulation results for the case without and with reconnection synchronization control also demonstrate significant improvements in the system’s transients with reconnection synchronization control. This also verified that the developed reconnection synchronization control works properly to smooth the angle change of the grid-forming inverter when the microgrid reconnects to the main grid.

## V. CONCLUSIONS

This paper presents an integrated synchronization control that smooths the angle change of a grid-forming inverter to operating within a microgrid during microgrid transition operation. This is shown to improve the microgrid’s transients and dynamics during microgrid transition operation. This integrated synchronization control includes the disconnection synchronization control and reconnection synchronization control. The detailed design and implementation of the integrated synchronization control is presented. Numerical simulation is performed in MATLAB/Simulink with an example microgrid to verify the proposed design compared to the conventional method without synchronization control. Two test cases including microgrid disconnection and reconnection operation are investigated. The simulation results show that the proposed synchronization control technique works effectively to smooth the angle change of the grid-forming inverter during microgrid transition operation. This improves the microgrid’s dynamic and transient performance compared to the case without synchronization control.

## ACKNOWLEDGMENTS

This work was supported by Alliance for Sustainable Energy, LLC, the manager and operator of the National Renewable Energy Laboratory for the U.S. Department of Energy (DOE) under Contract No. DE-AC36-08GO28308. Funding provided by the U.S. DOE, Office of Electricity Delivery and Energy Reliability. The views expressed in the article do not necessarily represent the views of the DOE or the U.S. Government. The U.S. Government retains and the publisher, by accepting the article for publication, acknowledges that the U.S. Government retains a nonexclusive, paid-up, irrevocable, worldwide license to publish or reproduce the published form of this work, or allow others to do so, for U.S. Government purposes.

## REFERENCES

- [1] Denholm, P., Ela, E., Kirby, B., Milligan, M., “The Role of energy storage with renewable electricity generation”, National Renewable Energy Laboratory, Golden, CO, Tech. Rep. NREL-TP-6A2-47187, 2010.
- [2] J. Wang, et al., “Design of an Advanced Energy Management System for Microgrid Controller Using a State Machine,” *Applied Energy* 228: 2407-2421, 2018.
- [3] J. Rocabert, et al., “Control of Power Converters in AC Microgrids,” *IEEE Trans. Power. Electron.*, vol. 27, no. 11, pp. 4734-4749, Nov. 2012.
- [4] I. J. Balaguer, et al., “Control for Grid-Connected and Intentional Islanding Operations of Distributed Power Generation,” *IEEE Tran. Ind. Electron.*, vol. 58, no. 1, pp. 147-157, January 2011.
- [5] C. Cho, et al., “Active Synchronization Control of a Microgrid,” *IEEE Tran. Power Electron.*, vol. 26, no. 12, pp. 3707-3719, Dec. 2011.
- [6] A. Micallef, et al., “Single-Phase Microgrid With Seamless Transition Capabilities Between Modes of Operation,” *IEEE Tran. Smart Grid*, vol. 6, no. 6, pp. 2736-275, Nov. 2015.
- [7] M. K. Ghartemani, “Universal Integrated Synchronization and Control for Single-Phase DC/AC Converters,” *IEEE Tran. Power Electron.*, vol. 30, no. 3, pp. 1544-1557, March 2015.
- [8] M. K. Ghartemani, et al., “Universal Controller for Three-Phase Inverters in a Microgrid,” *IEEE Tran. Emerging and Selected Topics in Power Electronics*, vol. 4, no. 4, pp. 1342-1353, Dec. 2016
- [9] Q. Zhong, et al., “Self-Synchronized Universal Droop Controller,” *IEEE Access*, vol. 4, pp. 7145-7153, Nov. 2016.
- [10] J. Wang, et al., “Design of a Generalized Control Algorithm for Parallel Inverters for Smooth Microgrid Transition Operation,” *IEEE Ind. Electron.*, vol. 62, no. 8, pp. 4900-4914, August 2015.
- [11] J. Wang, et al., “Design of a Microgrid Transition Controller I: For Smooth Transition Operation Under Normal Conditions,” *IEEE Innovative Smart Grid Technologies Conference Europe (ISGT-Europe)*, Torino, 26-29, Sept., 2017.